Journal of Hydrology 548 (2017) 524–535

Contents lists available at ScienceDirect

Journal of Hydrology

journal homepage: www.elsevier.com/locate/jhydrol

Research papers

Characterization of floods in the United States

Manabendra Saharia [a,b,d], Pierre-Emmanuel Kirstetter [a,b,c,*], Humberto Vergara [b,c,d], Jonathan J. Gourley [c], Yang Hong [a,b]

[a] School of Civil Engineering and Environmental Science, University of Oklahoma, Norman, OK 73072, USA
[b] Advanced Radar Research Center, University of Oklahoma, Norman, OK 73072, USA
[c] NOAA/National Severe Storms Laboratory, Norman, OK 73072, USA
[d] Cooperative Institute for Mesoscale Meteorological Studies, Norman, OK 73072, USA

ARTICLE INFO

Article history:
Received 12 February 2016
Received in revised form 7 January 2017
Accepted 6 March 2017
Available online 18 March 2017
This manuscript was handled by
K. Georgakakos, Editor-in-Chief, with the
assistance of Ercan Kahya, Associate Editor

Keywords:
Flood characterization
Geomorphology
Unit peak discharge
Flooding rise time

ABSTRACT

Floods have gained increasing global significance in the recent past due to their devastating nature and potential for causing significant economic and human losses. Until now, flood characterization studies in the United States have been limited due to the lack of a comprehensive database matching flood characteristics such as peak discharges and flood duration with geospatial and geomorphologic information. The availability of a representative and long archive of flooding events spanning 78 years over a variety of hydroclimatic regions results in a spatially and temporally comprehensive flood characterization over the continental U.S. This study, for the first time, employs a large-event database that is based on actual National Weather Service (NWS) definitions of floods instead of the frequently-adopted case study or frequentist approach, allowing us to base our findings on real definitions of floods. It examines flooding characteristics to identify how space and time scales of floods vary with climatic regimes and geomorphology. Flood events were characterized by linking flood response variables in gauged basins to spatially distributed variables describing climatology, geomorphology, and topography. The primary findings of this study are that the magnitude of flooding is highest is regions such as West Coast and southeastern U.S. which experience the most extraordinary precipitation. The seasonality of flooding varies greatly from maxima during the cool season on the West Coast, warm season in the desert Southwest, and early spring in the Southeast. The fastest responding events tend to be in steep basins of the arid Southwest caused by intense monsoon thunderstorms and steep terrain. The envelope curves of unit peak discharge are consistent with those reported for Europe and worldwide. But significant seasonal variability was observed in floods of the U.S. compared to Europe that is attributed to the diversity of causative rainfall ranging from synoptic scales with orographic enhancements in the West Coast, monsoon thunderstorms in the desert Southwest, to land-falling tropical storms and localized, intense thunderstorms in the Southeast.

1. Introduction

Floods are one of the most devastating natural disasters in the world that account for one-third of all global geophysical hazards (Smith and Ward, 1998; Adhikari et al., 2010). Floods, especially flash floods, have attracted significant attention in the recent past, both in academia and the wider world, due to their devastating nature and potential for causing substantial economic damage and loss of life. Flood hazard studies at the continental and global scales have received more attention as the destructive effects of flooding events are given more importance in public policy. According to the United States Flood Loss Report for Water Year 2014 (October 1, 2013 – September 30, 2014) compiled by the National Weather Service for the U.S. Army Corps of Engineers, the direct flood damages totaled $2.86 billion in the United States alone. Fifty-five flood-related deaths were recorded, out of which 29 were attributed to vehicle-related accidents and 39 to flash flood events (NWS, 2014). With ever increasing urbanization, casualties and damages due to flooding is expected to increase. Heavy precipitation is also seeing an upward trend at both continental (Groisman et al., 2004) and global scale (Groisman et al., 2005), which will increase the frequency and impact of flood hazards.

Floods and especially flash floods have not received the systematic and comprehensive study commensurate with their social and

* Corresponding author at: National Weather Center, 120 David L. Boren Blvd, Rm. 4706, Norman, OK 73072-7303, USA.
E-mail address: pierre.kirstetter@noaa.gov (P.-E. Kirstetter).

http://dx.doi.org/10.1016/j.jhydrol.2017.03.010
0022-1694/

economic impacts. To understand the spatial, temporal and geographic distribution of floods, we must first have a centralized database that collates quantitative information regarding floods. However, such databases are not easily available as formal records on previous floods are scattered across disparate sources. Due to this limitation, flood characterization studies have been performed mostly based on case studies or limited databases. Costa (1987) described the hydraulic characteristics of twelve of the largest floods of small basins ever measured by the U.S. Geological Survey (USGS) in the conterminous United States (CONUS) and related them to basin morphometry of the channels. He concluded that basin physiography and geology, in addition to rain intensity and duration, are major factors in maximizing runoff. In order to devise a procedure to distinguish flash floods from other floods, Bhaskar et al. (2000) developed a Flash Flood Index. The index utilizes characteristics describing the shape of the flood hydrograph and shows weak to moderate correlation with additional hydrograph variables such as unit peak discharge and direct runoff volume. Merz and Blöschl (2003) identified the causative mechanisms of floods using 11,518 maximum annual flood peaks in 490 Austrian catchments. Gaume et al. (2009) reported the compilation of an inventory containing 550 documented flash flood events in seven hydrometeorological regimes in Europe. Marchi et al. (2010) performed a detailed study of 25 selected extreme flash floods in Europe to identify causative processes and related them to climate and basin morphology. They characterized these events in terms of basin morphology, flood-generating rainfall, peak discharges, runoff coefficient, and response time to identify implications for flash flood risk management. To approximate the basin behavior in response to rainstorms, Perucca and Angilieri (2011) evaluated the flash flood hazard of del Molle basin in Argentina by analyzing different morphometric properties. The study reported the probability of a serious flash flood hazard in the basin and suggested implementation of mitigation measures.

In the United States, flood characterization has been done mostly through limited case studies or for a part of the country since the available information is usually sparse and non-homogeneous. Most flood databases do not catalogue sufficient information such as geospatial and geomorphologic data to be adequate for flood characterization studies. A comprehensive flood database should have certain information such as flood response variables (e.g. flooding rise time, recession time, etc.), peak discharge information, gridded rainfall rate data and as many geomorphologic parameters of the basins as possible in order to evaluate specific parameters that improve analysis of the driving geomorphologic and climatological factors, and hydrologic simulations. Some of the existing hazard databases that catalogue flooding events include the freely-accessible Emergency Disasters Database (EM-DAT) by the Center for Research on the Epidemiology of Disasters (CRED), that covers natural and man-made disasters from 1900-present (http://www.emdat.be/). The United Nations Office for the Coordination of Humanitarian Affairs (OCHA) also maintains ReliefWeb (http://www.reliefweb.int/) which publishes disaster reports in real-time. The International Flood Network (IFNET) publishes a flood event database based on voluntary submission of events that caused 50 or more casualties between 2005 and 2007 (http://www.internationalfloodnetwork.org/). The Dartmouth Flood Observatory (DFO) maintains a Global Archive of Large Flood Events (http://floodobservatory.colorado.edu/) which is one of the most comprehensive flood databases derived from a variety of sources such as remote sensing images and government reports (Brakenridge and Karnes, 1996). However, even though the database has good global coverage, it is not exhaustive enough and its events are only geo-referenced up to 2006, which limits its usability in evaluating and improving flood models. Adhikari et al. (2010) also reported a digitized global flood inventory (1998–2008) with georeferenced flooding events.

A recent effort was undertaken to build and make publicly available a Unified Flash Flood Database described in Gourley et al. (2013), which is used in this paper. It should be noted that the database incorporates all floods, including flash floods. The database comprises USGS streamflow measurements, storm reports collected by the National Weather Service (NWS), and public survey responses during the SHAVE experiment (Gourley et al., 2010). This dataset has undergone extensive post-processing to maintain consistency in data formats across the various sources. The long USGS component of the database is suitable for characterizing floods because it contains most of the necessary attributes such as flooding rise time, peak discharge, basin area, etc. The NWS, in collaboration with local stakeholders, has defined flooding thresholds for USGS stream gauge locations, which are used to extract flooding events from the streamflow record. Michaud et al. (2001) have depicted the distribution of large floods in the U.S. using data from 130 USGS stations, but only for basins less than 200 km^2. O'Connor and Costa (2004) was the first study to systematically analyze large portions of the USGS streamflow dataset comprising largest 10% of annual peak flows from 14,815 stations. While it states that specific basins of high unit peak discharge correspond to relatively high topographic relief, it only provides a qualitative assessment of this relationship due to unavailability of geomorphological data. Other studies have uncovered flooding characteristics in a portion of the country using the same USGS data, such as Villarini and Smith (2010) in the eastern U.S. and Mallakpour and Villarini (2015) in the central U.S. Smith and Smith (2015) used this dataset to identify the "flashiest" watersheds in the contiguous United States based on the frequency of discharge peaks exceeding 1 $m^3 s^{-1} km^{-2}$. They noted urban areas were frequently affected by flash flooding in the south-central U.S. (i.e., Tulsa, Oklahoma and St. Louis, Missouri) up through the mid-Atlantic (i.e., Baltimore, Maryland) as well as the Pacific Northwest. A recent study by Saharia et al. (2016) introduced a new variable called "flashiness" as a measure of flash flood severity which was extended and regionalized from gauged basins to a high resolution grid covering the CONUS. Benefiting from the representativeness and length of the Unified Flash Flood Database, the present study provides a spatially and temporally comprehensive flood characterization over the CONUS. This study, for the first time, employs a large-events database based on NWS definitions of floods instead of a frequently-adopted case study or frequentist approach, which allows us to base our analyses and conclusions on real definitions of floods. It examines flood regimes across the CONUS in order to determine how space and time scales of floods vary with climatic regimes, seasons, and geomorphology. This characterization of flood events paves the way towards improving hydrologic forecasting and risk management.

The purposes of this analysis are to (i) present an overview of the database that covers flooding events over more than 70 years from 1936 to 2013, (ii) characterize flooding events according to geomorphological basin attributes and climate classes, (iii) establish new relationships and envelope curves taking advantage of the lengthy historical record of floods, (iv) explore the results from the perspective of improving flood forecasting and risk management. The paper is organized as follows. Section 2 describes the flood and geomorphology database, the development of the archive, and an overview of the distribution of floods over the CONUS. Sections 3 and 4 characterize unit peak discharge and flooding rise time, respectively, based on geomorphologic parameters such as basin area, relief ratio, and shape factor. Finally, Section 5 provides a summary of findings and concluding remarks.

2. Study area and data used

The Unified Flash Flood Database aims at collating flooding information from various sources including streamflow measurements by the US Geological Survey (USGS), reports of flash flooding in the National Weather Service Storm Events Database, and public survey responses on flash flood impacts collected during the Severe Hazards Analysis and Verification Experiment (SHAVE) (Ortega et al., 2009; Gourley et al., 2010). With the combination of high-resolution details of SHAVE, spatial coverage of NWS reports and automated data collection with the USGS streamflow records, this database provides the most representative depiction of flash flooding in the United States. It is publicly available at: http://blog.nssl.noaa.gov/flash/database/.

In our study, we used the historical archive of automated streamflow measurements at USGS stations. Instantaneous streamflow recordings are collected at intervals ranging from 5 to 60 min for 10,106 gauges in the database. The NWS, in coordination with local stakeholders and the USGS, has defined stages corresponding to action, minor, moderate, and major flooding for 3490 stream gauge locations. Data from these stations are particularly useful given that the estimation of flooding thresholds has already been defined. One could rely on annual recurrence intervals in order to define thresholds for the stations without defined flood stages, but this introduces another source of uncertainty. The flood stage subset is further screened in order to eliminate gauges that have some degree of anthropogenic influence from regulation or diversion according to a data quality code that is supplied with the USGS peakflow data. The final data sample consists of 70,273 flooding events, defined as streamflow that exceeded that gauges' defined action stage, from 1642 gauges. According to the definitions and general terminology provided in the NWS manual 10–950-Hydrologic Services Program, action stage is "the stage which when reached by a rising stream, lake, or reservoir represents the level where the NWS or a partner/user needs to take some type of mitigation action in preparation for possible significant hydrologic activity" (http://www.nws.noaa.gov/directives/sym/pd01009050curr.pdf). Note that a subset of these gauges provide a stage corresponding to bank-full conditions; this bank-full stage is very similar to the action stage threshold used hereafter. For each event, the database provides the following information: the USGS Gauge ID, latitude (decimal degrees), longitude (decimal degrees), start time (UTC) at which the flow exceeded the action stage threshold, end time (UTC) when the flow dropped below the threshold, peakflow magnitude (m^3/s), time at which peakflow occurred (UTC), and the difference between the time at which the stream first exceeded action stage and reached its maximum flow, defined as the flood rise time (in hours). Variables such as flood duration, rise time and recession time were calculated systematically.

The flood characteristic database was enhanced with geomorphologic and climatological attributes specifically derived for each basin in this study. We include parameters that potentially influence the evolution of a flood in space and time. For example, smaller basin area leads to shorter flooding rise times as water takes less time to travel through the watershed. They were derived from Digital Elevation Model (DEM) data from the National Elevation Dataset (NED; http://ned.usgs.gov); more details concerning how they are computed are provided in section 3. All basins were delineated with USGS stations to prepare the flow accumulation and flow direction information. It was checked by resampling the 30-m DEM to a 1-km grid using the National Hydrography Dataset (NHD; http://nhd.usgs.gov) to verify that DEM-based flow accumulation computations agree with the actual river network across the CONUS. Hydroclimatic variables such as annual precipitation was extracted from the 30-year climatological datasets released by the PRISM climate group (http://www.prism.oregonstate.edu/normals/) of Oregon State University from 1981 to 2010. Custom libraries developed in MATLAB were then utilized to derive the parameters based on the resulting grid-based delineated catchments.

3. Spatial and temporal distribution of floods

In order to investigate the potential dependence of floods on climatic regime, the analysis used the Köppen-Geiger Climate Classification over the U.S given in Kottek et al. (2006). Fig. 1 shows the distribution of all USGS stations in the database over the CONUS segregated according to the Köppen-Geiger climate classes. Six classes were utilized in this study: Warm temperate fully humid extremely continental (Cfa), Warm temperate summer dry warm summer (Csb), snow fully humid hot summer (Dfa), snow fully humid warm summer (Dfb, West and East) and Arid steppe cold arid (BSk). The number of flooding events and gauges in each climate class is given in Table 1, along with the number of flooding events normalized by the number of gauges in each regime to enable comparison between different climate classes. Cfa has the highest number of 39,872 events while Dfb (W) has the lowest with 905 events. Basins in the eastern half of U.S. that comprises of Dfb (E), Dfa, and Cfa have higher number of flooding events per gauge than the western half of U.S. comprising Csb, BSk, and Dfb (W).

Precipitation, being the primary driver of floods, is important to explain the variability of flooding events. The summary statistics for average annual precipitation computed for the six climate classes is provided using the box-and-whisker plot of Fig. 2. The band inside the box is the second quartile (median), while the bottom and top of the boxes correspond to the first (25th percentile) and third quartiles (75th percentile), respectively. The mean is given by the open circle inside the box. The whiskers extend to the extremes of the observations and outliers outside 1.5 times the inter-quartile range are plotted as filled circles. The highest annual precipitation of 1537 mm/y falls in the Csb region, which is expected as moisture-laden westerlies from the ocean encounter the high mountain ranges of California, Oregon, and Washington, including the Olympic Mountains, the Cascades, and the Sierra Nevada range. After Csb, areas in the East such as the southeastern US (Cfa), eastern and midwestern US from the Atlantic to the 100th meridian (Dfa) and the Great Lakes region with New England (Dfb (E)) experience high precipitation. The semi-arid region of BSk that acts as a transition zone between humid and desert climate has the lowest annual precipitation among the six classes, while the Dfb (W) region that contains the Rocky Mountain range receives slightly higher precipitation.

Even though the dataset spans 78 years, a majority of the data (92.9% of events) is concentrated in the last two decades. The number of gauges also doesn't remain constant during this period. So, to detect any temporal trend in the most extreme floods, the number of major stage floods in each year were normalized by the number of action stage floods for the past three decades. This was performed on the dataset for the CONUS as well as for the different climate classes. No clear trend was observed nationally; however, Dfb (E) suggests an increasing trend as shown in Fig. 3. A similar increasing trend in annual maximum daily flow was observed in the northeastern U.S. by Lins and Slack (1999) that was attributed to precipitation patterns linked with the persistent high index phase of the North Atlantic Oscillation at that time. However, a detailed analysis of this trend would need additional studies involving climate datasets and is beyond the scope of this paper.

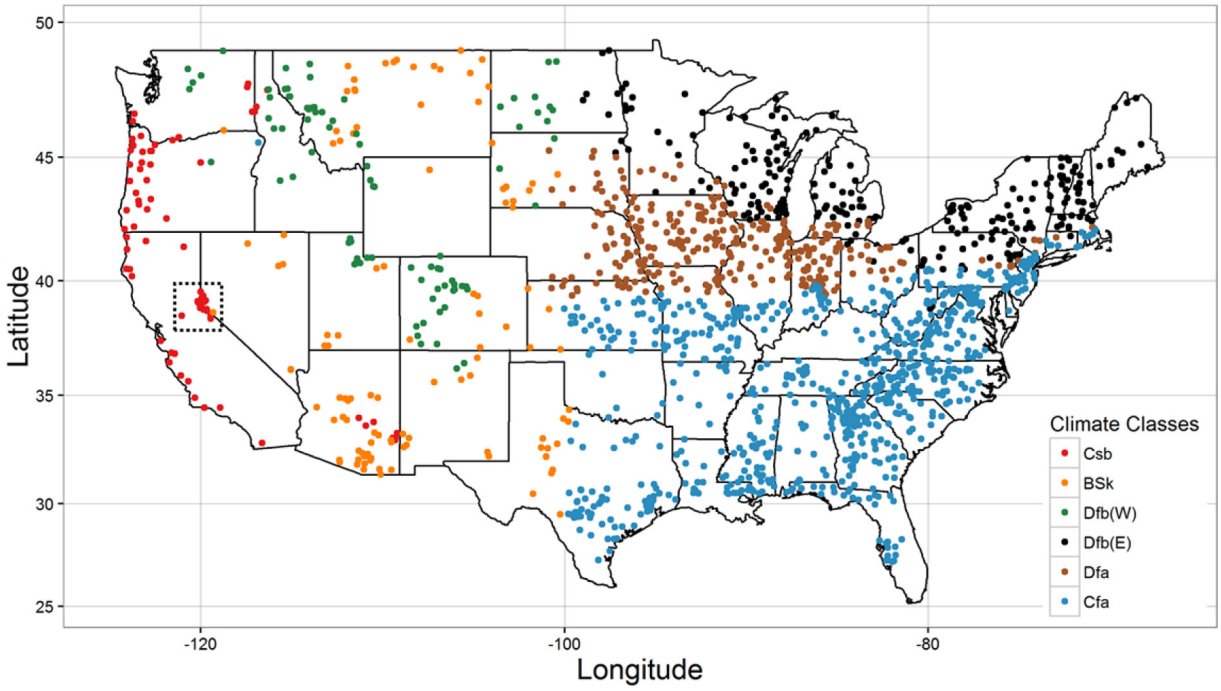

Fig. 1. Distribution of USGS streamflow stations used in this study color-coded by Köppen-Geiger Climate Classes. The black box within the Csb region is a sub-class called Csb 1 and the rest of Csb outside the box is termed Csb 2 in this study.

Table 1
Number of flooding events and gauges in each climate class along with normalized values of number of flooding events. Floods are defined by discharge exceeding action stage, as defined by National Weather Service employees and local stakeholders.

Climate Classes	Flooding events	Gauges	Flooding events/Gauges
Csb	1688	78	21.64
BSk	1129	110	10.26
Dfb (W)	905	84	10.77
Dfb (E)	9901	230	43.05
Dfa	16778	313	53.60
Cfa	39872	827	48.21

The regional variations of flood frequency are evaluated on a monthly basis for a better understanding of flood dynamics and the driving factors. Fig. 4 shows the monthly distribution of flooding events normalized by the total number of events in the various climate classes. The northern migration of the jet stream during the winter brings most of the precipitation to the West Coast, which experiences the highest number of flooding events among all classes during the November-March period. Michaud et al. (2001) found that as one moves inland, the primary flood season shifts to the warm season: late spring/early summer in the northern intermountain West and late summer in the more southerly monsoon-dominated regions. The monthly frequency confirms this, as the other climate classes experience more flooding events than the West Coast during the warm season. The intermountain West in the Dfb (W) region experiences a high number of floods during the onset of the warm season (April-July) while the semi-arid region of BSk, which receives monsoon precipitation, experiences the highest number of floods in the late summer months (June-September). Basins in the Great Lakes region of Dfb

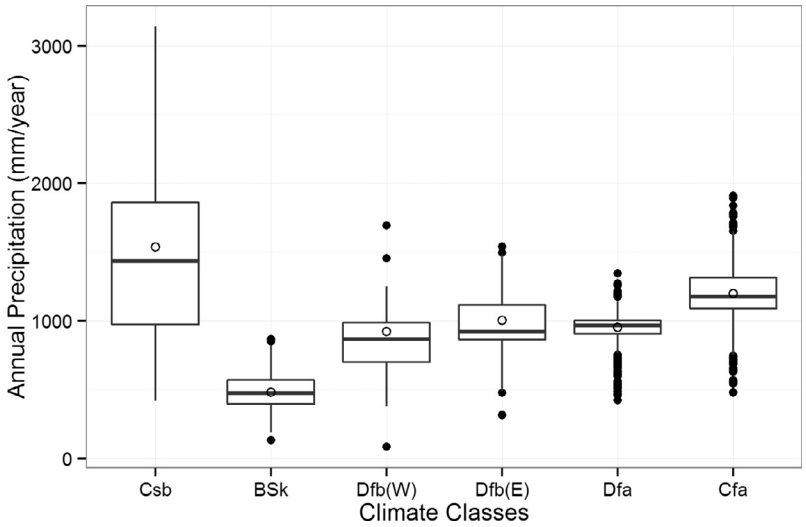

Fig. 2. Box-and-whisker plot of annual precipitation in different climate classes.

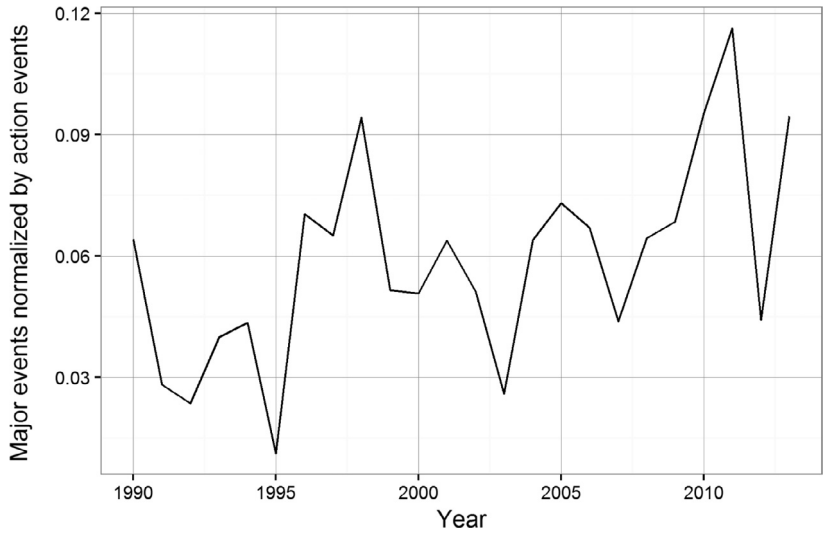

Fig. 3. Temporal evolution of the number of the events that exceeded major flood stage divided by the number of action stage events each year for Dfb (E).

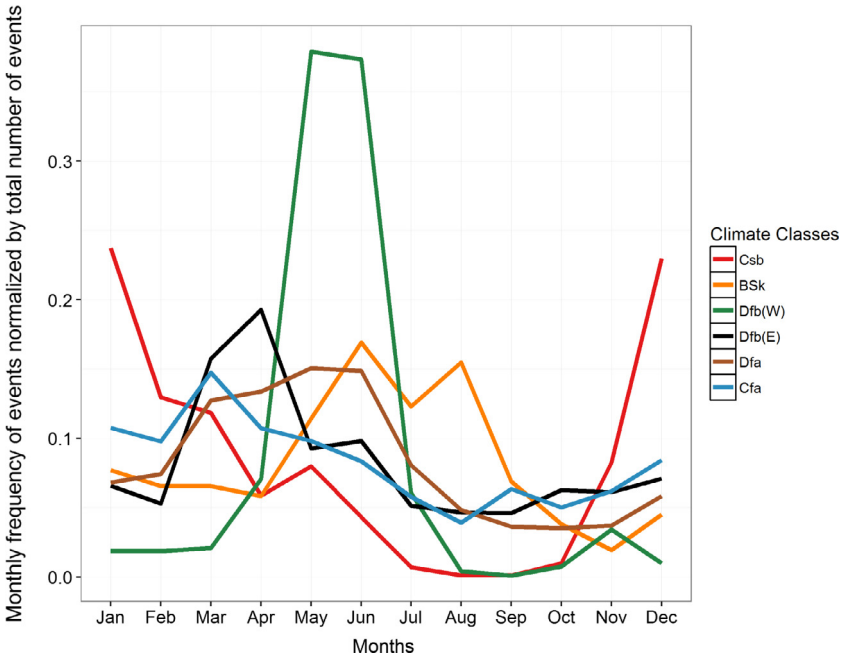

Fig. 4. Monthly distribution of flooding events normalized by the total number of events in different climate classes.

(E) have a tendency to be flooded more during the spring season while the Southeast in Cfa shows the lowest monthly variation of flooding, with a higher tendency of being flooded in early spring.

The number of flooding events in a climate class is correlated with the average annual precipitation given in Fig. 2. With the exception of Csb, which is driven by synoptic-scale precipitation events during the cool season, the next two classes experiencing the highest annual average precipitation, Cfa and Dfa, get the largest number of floods during spring and early summer. As we move westward to basins in Dfb (W) and BSk, deep moist convection plays a larger role with the occurrence of highest number of floods occurring in late-spring and summer.

4. Characterization of floods based on physiographic factors

The terrain of a catchment influences catchment response through the combined effects of orography on precipitation rates and topographic relief on streamflow evolution. Geomorphologic analysis is thus of vital importance in describing the hydrologic behavior of basins as it influences factors such as response times and peak discharge values. Relationships between flooding variables and geomorphological parameters are very useful in modeling as geomorphology changes very slowly and most of these parameters can be easily calculated from DEM data. Studies such as Collier and Fox (2003) and Collier (2007) identified several morphological characteristics such as catchment slope and ratio of catchment area to mean drainage path length that have a large correlation with basin susceptibility to flooding. Apart from exploring the general interdependence between flooding variables and basin area, this study also explores several other variables such as relief ratio and shape factor to determine how various basins respond in different regions.

The relief ratio is the ratio between the total relief of a basin (elevation difference of lowest and highest points of a basin) and

the longest dimension of the basin parallel to the principal drainage line (Schumm, 1956). This dimensionless height-length ratio allows for comparison of relative relief of basins with varying topography. We can generally anticipate that a higher relief ratio would be associated with a basin more prone to flooding with faster concentration of streamflow. Higher terrain gradients with generally shallow soils imply that a greater proportion of the water becomes infiltration-excess runoff, while runoff is more likely to be saturation-excess in gently sloping basins. The relation between relief ratio and basin area for different climate classes is given in Fig. 5. The general relationship of decreasing basin relief with increasing basin area is in conformity with reported literature (Dade, 2001; Marchi et al., 2010).

The summary for values of relief ratio over the six climate classes is given by the box-and-whisker plot of Fig. 6. Values of relief ratio over the CONUS range from 0.0002 to 0.17, with an average value of 0.008 which is comparable to values reported in other studies (Costa, 1987; Marchi et al., 2010). From the box-and-whiskers plots, it can be seen that basins in the western half of the CONUS, i.e. West Coast (Csb), Rocky Mountains (Dfb (W)) and the intermountain West (BSk) have higher average relief ratio values than the basins in the eastern half (Dfa, Dfb (E) and Cfa). The highest mean values of relief ratio are found in the Rocky Mountain range of Dfb (W) and the West Coast (Csb), both of which also experience some of the highest number of flooding events in the CONUS (Fig. 4). The lowest value is in Dfa, which covers a majority of the Midwest (High Plains).

5. Characterization of floods based on flood response

The relationship between peak discharge and basin area is well-understood and has been explored in several studies (Furey and Gupta, 2005; Gupta et al., 1996; Marchi et al., 2010; Smith, 1992; among others). A strong correlation between drainage area and discharge is intuitive as it is expected that channels in larger catchments will collect and carry proportionately larger discharges. This relationship will be linear if the unit peak discharge (i.e. the ratio between peak discharge and upstream basin area) is spatially constant. However, in reality, spatial heterogeneity is introduced in the amount of peak discharge per unit area by various factors such as slope, vegetation, rainfall intensity, and spatial rainfall coverage over the basin, etc. The peak discharge values in this study vary greatly in magnitude as the basin sizes vary over several orders of magnitude from 3.68 km^2 to 1,061,895 km^2. Figs. 7 and 8 show the summary statistics of unit peak discharges and basin area respectively for the six climate classes. Both the highest median unit peak discharge and smallest basin area occurs in West Coast (Csb).

Envelope curves provide an effective summary of historical floods in a study area and have been widely used in previous studies on extreme floods (Jarvis, 1926; Crippen and Bue, 1977; Herschy, 2002; Castellarin, 2007). The dependence between basin area and unit peak discharge for each climate class is explored using log-log diagrams, envelope curves and quantile plots. A simple power-law formula (Eq. (1)) used in previous studies is selected here.

$$Q_u = \alpha A^{\beta} \quad (1)$$

where Q_u is the unit peak discharge ($m^3\ s^{-1}\ km^{-2}$), A is the contributing basin area (km^2), coefficient α is known as reduced discharge and β is a scaling coefficient (Gaume et al., 2009). The values of α and β were determined by fitting a regression line between log (Q_u) and log (A) values for each climate class. The regression was computed on the entire sample and shifted to identify the upper envelope. While α is independent of A, the constant β represents the degree to which unit peak discharge varies with basin area. Atmospheric humidity and surface characteristics affect the unit peak discharge values of basins. The lower the value of β, the faster the proportionate decrease of unit peak discharge with the contributing basin area.

The envelope curves are the straight lines on the log-log diagram developed for different levels of floods and each climate class that can be seen in Figs. 9 and 10, respectively. The National Weather Service has defined flood stage levels in gauging stations across the country such as action, minor, moderate and major stage. Flood levels exceeding action stage are closely related to bank-full conditions and require the authorities to start taking mitigation procedures for possible flooding; minor stage causes minimal property damage; moderate stage causes some inundation in roadside structures and roads near streams; and major stage causes extensive inundation of structures and roads. The solid lines in Fig. 9 are the envelope curves for the four levels of floods in CONUS and the dotted line is the envelope curve for major floods in Europe ($Q_u = 97.0\ A^{-0.4}$) for comparison, as proposed in Gaume et al. (2009).

Table 2 gives α and β values of the CONUS-wide envelope curves for the four flood stages and the exponent (β) in the

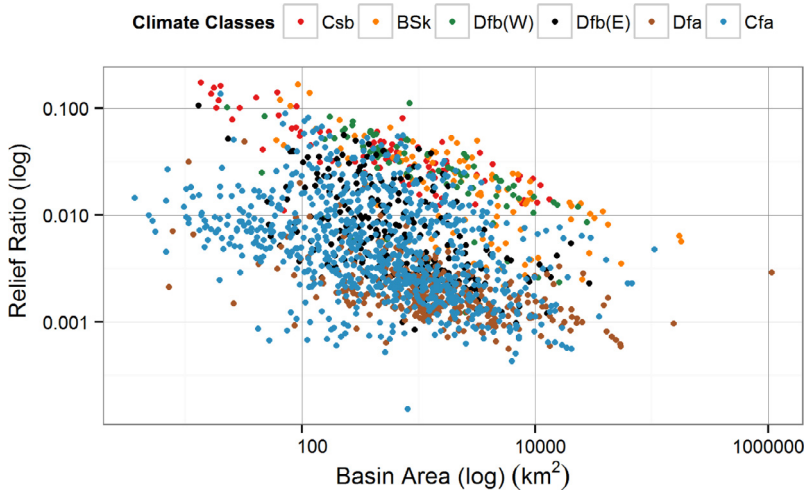

Fig. 5. Relief ratio plotted as a function of basin area where the colors correspond to different climate classes (refer to legend). The sample size of each climate class is reported in Table 1.

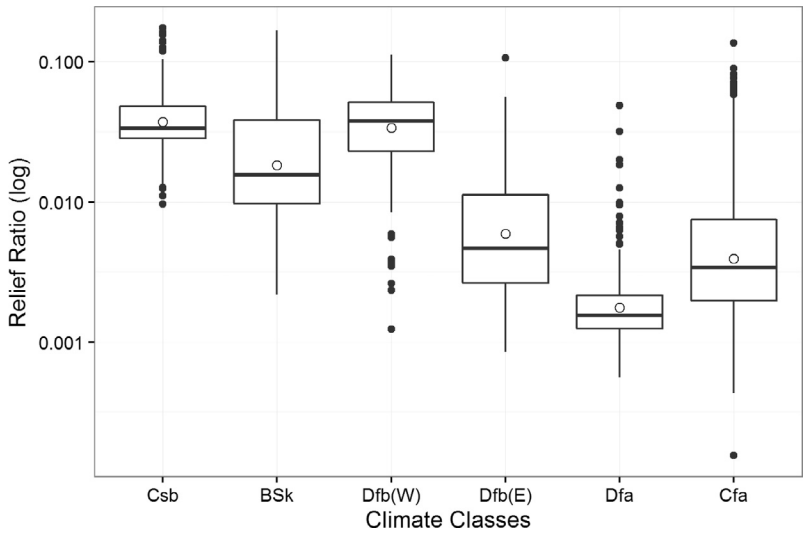

Fig. 6. Box-and-whisker plot of relief ratio in different climate classes. The horizontal line within the box is the second quartile (median), the open circle is the mean, and the bottom and top of the boxes correspond to the first (25th percentile) and third quartile (75th percentile) respectively. The whiskers extend to the extreme values and filled circles are the outliers outside 1.5 times the inter-quartile range.

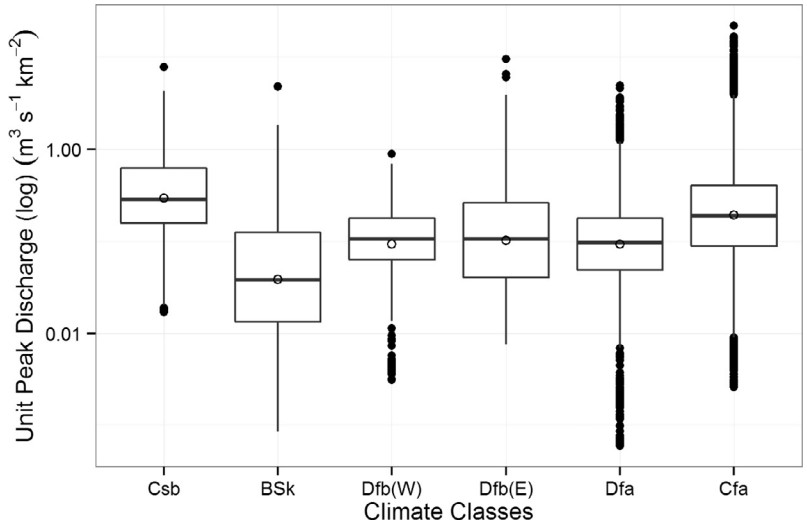

Fig. 7. Box-and-whisker plot of unit peak discharge in different climate classes.

power-law relationship varies according to stage. The most extreme floods in the CONUS corresponding to the major stage have a β value of −0.44, which is very near to the value of −0.40 proposed for European extreme floods by Gaume et al. (2009) and Marchi et al. (2010). This can also be seen in Fig. 9, where the solid line corresponding to the major stage is nearest to the European envelope curve. The reported β value for major stage floods in CONUS is greater than the value of −0.643 proposed for global extreme floods (Herschy and Fairbridge, 1998) and −0.57 for mostly riverine floods in Europe (Herschy, 2002). Nonetheless, the asymptotic increase of the envelope curves derived in this study with increasing flood severity toward the European curve supports the argument that there is a global envelope or upper limit to unit peak discharges.

Table 3 gives α and β values of the envelope curves according to climate classes. While some of the values are comparable, the range of basin areas as well as sample sizes is greater in this study than in the European studies (Gaume et al., 2009; Herschy, 2002; Marchi et al., 2010). Within the CONUS, the approximate value of β is highest for Csb class (−0.081) and lowest for BSk (−0.501). With the lowest annual average precipitation (479 mm/yr) as well as lowest annual maximum rainfall (866 mm/yr) as given in Fig. 2, the arid basins in the BSk class experience the most drastic reduction in unit peak discharge values with basin area compared to other classes. Basins in the West Coast of the U.S. falling in climate class Csb have the highest annual average rainfall (1537 mm/yr) among the six classes which results in higher values of unit peak discharge, and these basins show the slowest decrease in unit peak discharge values with basin size. Upon further analysis, a discontinuity in range of basin areas of in West Coast was observed. On dividing the events based on a 250-km^2 threshold, the two areas were found to be geographically distinct where the larger basins were located in Coastal California (Csb 1) and the smaller basins were mostly in the Sierra Nevada mountain range along with some isolated basins in Northern and Southern California (Csb 2). The basins in Csb 1 with an average size of 1700 km^2 are much larger than those in Csb 2 with an average basin size of 77 km^2. Computing the envelope curves for these two sub-regions, we get β values

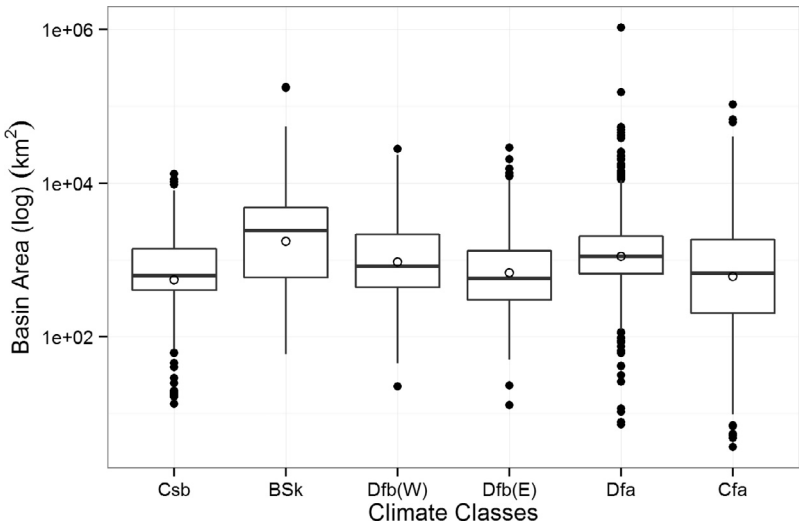

Fig. 8. Box-and-whisker plot of basin area in different climate classes.

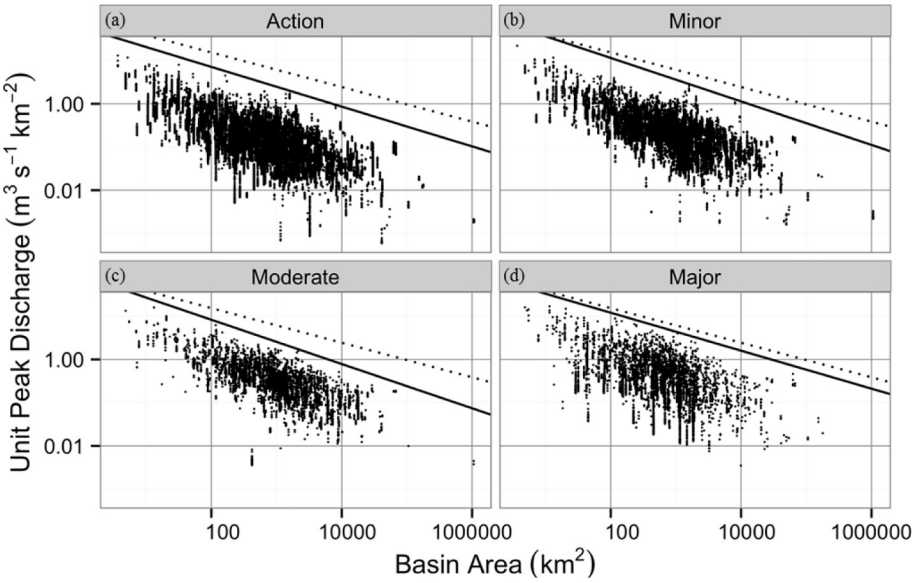

Fig. 9. Unit peak discharges versus basin area along with their CONUS-wide envelope curves for (a) action, (b) minor, (c) moderate and (d) major stage floods. The solid line is for CONUS-wide envelope curves while the dotted line is the envelope curve for 25 extreme floods across Europe as reported in Marchi et al. (2010).

of −0.56 for Csb 1 and −0.31 for Csb 2. Interestingly, the unit peak discharges in basins with contributing areas less than 100 km^2 of BSk and Csb are similar. This means that flash flooding resulting from intense, convective cells in these arid basins results in similar peakflows as those experienced in the Pacific Northwest that receive much more rainfall on average. However, the unit peak discharges in BSk at larger scales (>100 km^2) are much lower due to the influence of drier surface conditions, evaporation, and the smaller space-time scales of the causative precipitation systems. Basins in the eastern half of the CONUS exhibit similar values of β, but there is a general increase in α going from north to south. This means that the effective scales of the causative rainfall have similar characteristics in the east with increasing rainfall intensities as one moves south.

In comparison to floods in Europe reported in Gaume et al. (2009) and Marchi et al. (2010), we find similarities in the following characteristics. First, the highest unit peak discharges tend to occur in basins in close proximity to the ocean that also have mountainous terrain. These conditions are met both in the Cevennes-Vivarais region of the Mediterranean and also along the West Coast of the US. The seasonality of the events are different, however, with the Mediterranean ones generally occurring in autumn and the West Coast events occurring in the cool season. Similar to Europe, the unit peak discharges generally decrease moving inland. The dependence of unit peak discharge on basin area is attributed to the spatial scales of the rainfall forcing that can be exacerbated by evaporation and dry surface conditions. The U.S. has some regions that are quite distinct from Europe. In particular, the BSk region of the desert Southwest is influenced by warm season, monsoon rainfall that exhibits very high unit peak discharges that depend strongly on basin area. Finally, the largest unit peak discharges in the U.S. occur in the Cfa region of the Southeast. Some basins are situated in the Appalachian mountains but this large class includes a wide variety of surface characteristics including plains. The causative rainfall in this most extreme class is also variable ranging from land-falling tropical storms from

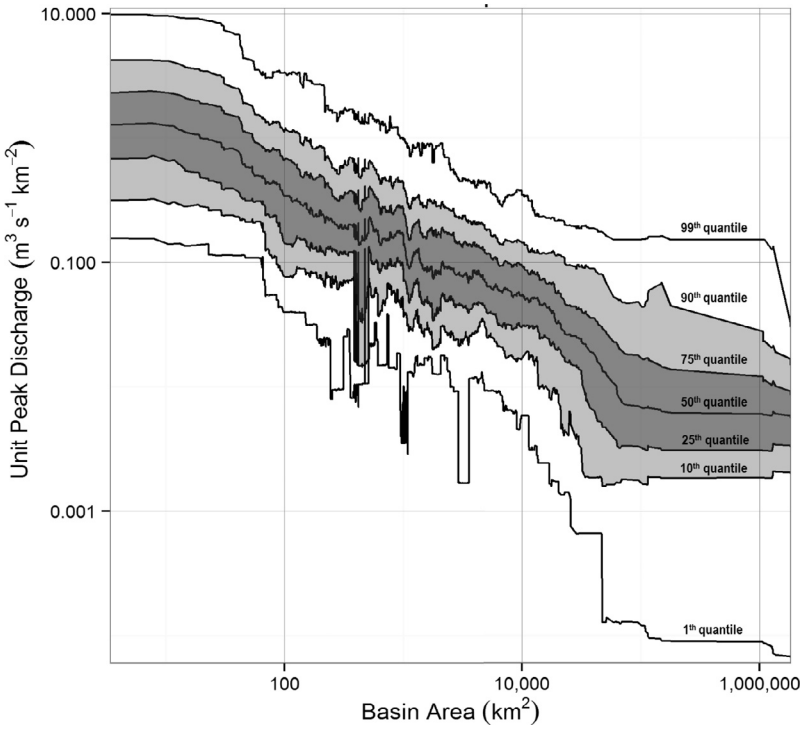

Fig. 11. Quantiles (10-90th percentile) of unit peak discharges versus basin area for all 70,273 flooding events spanning 78 years over the CONUS.

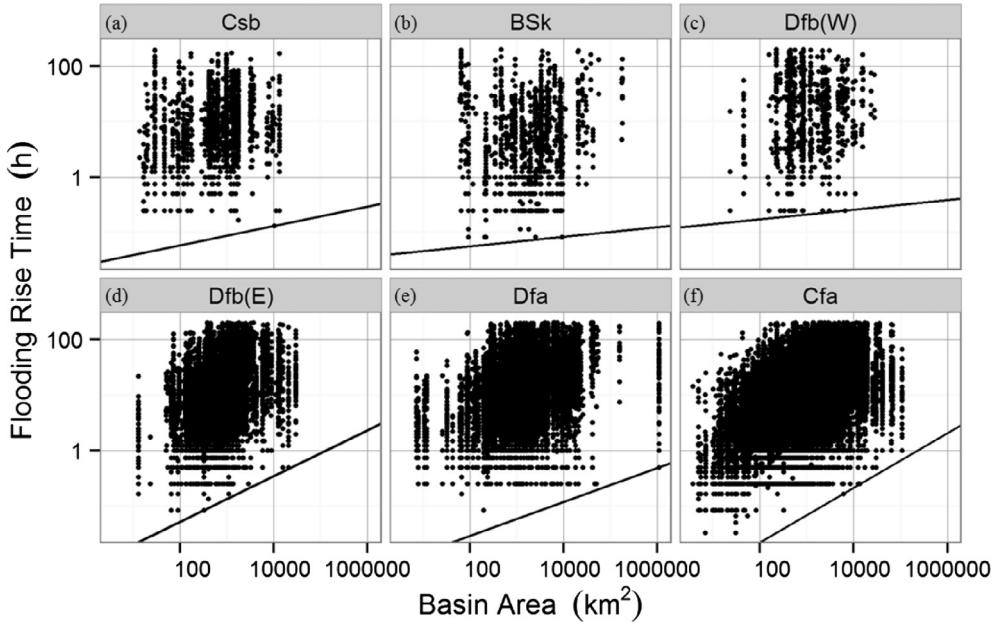

Fig. 12. Flooding rise times versus basin area along with their envelope curves for the (a) warm temperate summer dry warm summer (Csb) (b) arid steppe cold arid (BSk), (c) snow fully humid warm summer west (Dfb(W)), (d) snow fully humid warm summer east (Dfb(E)), (e) snow fully humid hot summer, and (f) warm temperate fully humid extremely continental (Cfa) climate classes.

of values of flooding rise time with an average value of 20.6 h and a median of 10 h. Fig. 12 reports the relationship between flooding rise time and basin area for the six climate classes. The lower bounded curve enclosing all flooding rise times for each value of watershed area was derived, similar to what was derived for lag time in Marchi et al. (2010).

A power-law relationship (Eq. (2)) was used to represent the lowest bound of flooding rise time T_r (h) versus basin area (km^2).

$$T_R = \alpha A^{\beta} \quad (2)$$

where β is a scaling coefficient. The values of α and β were determined by fitting a regression line between log (T_r) and log (A) values for each climate class.

Table 3 gives the α and β values for the various climate classes as well as CONUS. Higher values of the β exponent indicate a faster increase of flooding rise time with basin area. The β value is the

highest for Cfa (0.493) and lowest for Csb 1 (0.042). Fig. 12 shows that the time at which floods reach their peak values after exceeding flood stage occurs more quickly at small basin scales, as one would expect. Examination of the scatter plots, envelope curves, and β values reveal a distinction between basins in the western (Csb, Csb 1, Csb 2, BSk, and Dfb(W)) and eastern half of the U.S. (Dfb(E), Dfa, and Cfa). Basins in the eastern half of U.S. with β values of 0.042–0.174 exhibit faster increases in flooding rise times with basin area than in western half with β values of 0.307–0.493. The arid intermountain West BSk stations tend to have quicker flooding rise times for a given basin area. This is most likely a result of the causative precipitation from intense convective cells that yield quick-responding flash floods during the monsoon. Further, many of the BSk stations are situated in steep terrain which contributes to these fast responses. In contrast, the Dfb (W) stations are not significantly displaced geographically from the BSk stations, but they are at much higher altitude. The high data density at slow flooding rise times is interpreted to be a result of snowmelt influences on flood peaks. Snowmelt generally occurs more gradually as compared to stream response to intense convective cells and likely explains this discrepancy. This inference is supported by Fig. 4, which shows that the Dfb (W) floods tend to occur earlier in the late spring months as compared to Bsk. The West Coast (Csb) consists of two distinct sub-regions based on basin area and events in Csb1, which is mostly the mountainous Sierra Nevada range, have very small exponent value of 0.042, which is a reflection of the small size of basins in this sub-region. While Csb2 has a slightly higher value of 0.174 as the basins are bigger than those in Csb1.

7. Conclusions

A systematic analysis of spatial and temporal characteristics of floods in the United States was performed based on USGS observations combined with NWS flood stage thresholds. Flood thresholds were studied to explore the influence of geomorphology and climatology. Flooding variables investigated are the unit peak discharge and the flooding rise time. The results are summarized as follows:

- Regions such as the West Coast (Csb) and southeastern United States (Cfa), which experience the most extraordinary precipitation, have the highest unit peak discharges. The dependence of unit peak discharge on basin area is determined by the spatial scales of the causative rainfall as well as the atmospheric humidity and aridity of the basin's soils.
- Analysis of the monthly frequency of flood events shows great variations among the different climate classes. While the West Coast experiences the highest number of floods during the cool season, the peak flood season shifts towards the warmer months as one moves further inland to basins within the Intermountain West.
- Unit peak discharge and flooding rise time depend on catchment area for all the climate classes. In mountainous areas, especially in the Rocky Mountains, relief has a greater impact on both unit peak discharge and rise time than basin area.
- The envelope curves developed for unit peak discharges and basin area are consistent with the studies of floods in Europe and worldwide. In general, the magnitude of the unit peak discharges depends on the causative rainfall, which tends to be more intense in the Southeast U.S. and the West Coast. The unit peak discharges of floods in the monsoon-dominated desert Southwest are modulated by dry atmospheric and land surface conditions, which becomes more apparent with increasing basin scale. Finally, the seasonality of the U.S. floods is quite variable compared to Europe. This variability is attributed to the diversity of flood-causing storms ranging from rainfall organized at synoptic scales but with orographic enhancements in the West Coast during the cool season to monsoon thunderstorms during the warm season in the desert Southwest to land-falling tropical storms and localized, intense thunderstorms in the Southeast.
- Flooding rise times are quickest in the desert Southwest (BSk) due to the coincidence of intense thunderstorms and steep terrain. Basins in the nearby Dfb (W) Intermountain West region are much slower to respond, presumably due to the influence of snowmelt.

This study proposes a general picture of the flood characteristics over the U.S. As a continuation, we will employ more sophisticated modeling techniques to analyze the impact of variables such as shape factor, curve number, event-scale precipitation variability indices, etc. on the flooding variables. This analysis framework is the basis to evaluate the behavior of distributed hydrologic model simulations such as the Flooded Locations And Simulated Hydrographs Project (FLASH) (http://flash.ou.edu, Gourley et al., 2016) under a variety of conditions. The eventual goal is to use this dataset to make better prediction of floods in the vast number of ungauged basins.

Acknowledgements

This work was supported by the Disaster Relief Appropriations Act of 2013 (P.L. 113-2), which funded the United States National Oceanic and Atmospheric Administration (NOAA) research grant NA14OAR4830100.

References

Adhikari, P., Hong, Y., Douglas, K.R., Kirschbaum, D.B., Gourley, J., Adler, R., Brakenridge, G.R., 2010. A digitized global flood inventory (1998–2008): compilation and preliminary results. Nat. Hazards 55, 405–422. http://dx.doi.org/10.1007/s11069-010-9537-2.

Bhaskar, N., French, M., Kyiamah, G., 2000. Characterization of flash floods in Eastern Kentucky. J. Hydrol. Eng. 5, 327–331. http://dx.doi.org/10.1061/(ASCE)1084-0699(2000) 5:3(327).

Brakenridge, G.R., Karnes, D., 1996. The Dartmouth Flood Observatory: an electronic research tool and electronic archive for investigations of extreme flood events. In: Geoscience Information Society Proceedings. Presented at the Geological Society of America Annual Meeting.

Castellarin, A., 2007. Probabilistic envelope curves for design flood estimation at ungauged sites. Water Resour. Res. 43, W04406. http://dx.doi.org/10.1029/2005WR004384.

Collier, C.G., 2007. Flash flood forecasting: what are the limits of predictability? Q. J. R. Meteorol. Soc. 133, 3–23. http://dx.doi.org/10.1002/qj.29.

Collier, C.G., Fox, N.I., 2003. Assessing the flooding susceptibility of river catchments to extreme rainfall in the United Kingdom. Int. J. River Basin Manag. 1, 225–235. http://dx.doi.org/10.1080/15715124.2003.9635209.

Costa, J.E., 1987. Hydraulics and basin morphometry of the largest flash floods in the conterminous United States. J. Hydrol. 93, 313–338. http://dx.doi.org/10.1016/0022-1694(87)90102-8.

Creutin, J.D., Borga, M., Gruntfest, E., Lutoff, C., Zoccatelli, D., Ruin, I., 2013. A space and time framework for analyzing human anticipation of flash floods. J. Hydrol. 482, 14–24. http://dx.doi.org/10.1016/j.jhydrol.2012.11.009.

Crippen, J.R., Bue, C.D., 1977. Maximum Floodflows in the Conterminous United States (No. WSP-1887). United States Geological Survey.

Dade, W.B., 2001. Multiple scales in river basin morphology. Am. J. Sci. 301, 60–73. http://dx.doi.org/10.2475/ajs.301.1.60.

Furey, P.R., Gupta, V.K., 2005. Effects of excess rainfall on the temporal variability of observed peak-discharge power laws. Adv. Water Resour. 28, 1240–1253. http://dx.doi.org/10.1016/j.advwatres.2005.03.014.

Gaume, E., Bain, V., Bernardara, P., Newinger, O., Barbuc, M., Bateman, A., Blaškovičová, L., Blöschl, G., Borga, M., Dumitrescu, A., Daliakopoulos, I., Garcia, J., Irimescu, A., Kohnova, S., Koutroulis, A., Marchi, L., Matreata, S., Medina, V., Preciso, E., Sempere-Torres, D., Stancalie, G., Szolgay, J., Tsanis, I., Velasco, D., Viglione, A., 2009. A compilation of data on European flash floods. J. Hydrol. 367, 70–78. http://dx.doi.org/10.1016/j.jhydrol.2008.12.028.

Gourley, J., Flamig, Z.L., Vergara, H., Kirstetter, P.-E., Clark, R., Argyle, A.A., Martinaitis, S., Terti, G., Erlingis, J.M., Hong, Y., Howard, K., 2016. Flooded locations and simulated hydrographs (FLASH) project: improving the tools for flash flood monitoring and prediction across the United States. Bull. Am. Meteorol. Soc.

Gourley, J.J., Erlingis, J.M., Smith, T.M., Ortega, K.L., Hong, Y., 2010. Remote collection and analysis of witness reports on flash floods: flash floods: observations and analysis of hydrometeorological controls. J. Hydrol. 394, 53–62. http://dx.doi.org/10.1016/j.jhydrol.2010.05.042.

Gourley, J.J., Hong, Y., Flamig, Z.L., Arthur, A., Clark, R., Calianno, M., Ruin, I., Ortel, T., Wieczorek, M.E., Kirstetter, P.-E., Clark, E., Krajewski, W.F., 2013. A unified flash flood database across the United States. Bull. Am. Meteorol. Soc. 94, 799–805. http://dx.doi.org/10.1175/BAMS-D-12-00198.1.

Groisman, P.Y., Knight, R.W., Easterling, D.R., Karl, T.R., Hegerl, G.C., Razuvaev, V.N., 2005. Trends in intense precipitation in the climate record. J. Clim. 18, 1326–1350. http://dx.doi.org/10.1175/JCLI3339.1.

Groisman, P.Y., Knight, R.W., Karl, T.R., Easterling, D.R., Sun, B., Lawrimore, J.H., 2004. Contemporary changes of the hydrological cycle over the contiguous United States: trends derived from in situ observations. J. Hydrometeorol. 5, 64–85. http://dx.doi.org/10.1175/1525-7541(2004) 005∗0064:CCOTHC∗2.0.CO;2.

Gupta, V.K., Castro, S.L., Over, T.M., 1996. On scaling exponents of spatial peak flows from rainfall and river network geometry: fractals, scaling and nonlinear variability in hydrology. J. Hydrol. 187, 81–104. http://dx.doi.org/10.1016/S0022-1694(96)03088-0.

Herschy, R.W., 2002. The world's maximum observed floods. Flow Meas. Instrum. 13, 231–235. http://dx.doi.org/10.1016/S0955-5986(02)00054-7.

Herschy, R.W., Fairbridge, R.W., 1998. Encyclopedia of Hydrology and Water Resources. Springer Science & Business Media.

Jarvis, C.S., 1926. Flood flow characteristics. Trans. Am. Soc. Civ. Eng. 89, 985–1032.

Kottek, M., Grieser, J., Beck, C., Rudolf, B., Rubel, F., 2006. World Map of the Köppen-Geiger climate classification updated. Meteorol. Z. 15, 259–263. http://dx.doi.org/10.1127/0941-2948/2006/0130.

Lins, H.F., Slack, J.R., 1999. Streamflow trends in the United States. Geophys. Res. Lett. 26, 227–230. http://dx.doi.org/10.1029/1998GL900291.

Mallakpour, I., Villarini, G., 2015. The changing nature of flooding across the central United States. Nat. Clim. Change. http://dx.doi.org/10.1038/nclimate2516 (advance online publication).

Marchi, L., Borga, M., Preciso, E., Gaume, E., 2010. Characterisation of selected extreme flash floods in Europe and implications for flood risk management: flash floods: observations and analysis of hydrometeorological controls. J. Hydrol. 394, 118–133. http://dx.doi.org/10.1016/j.jhydrol.2010.07.017.

Merz, R., Blöschl, G., 2003. A process typology of regional floods. Water Resour. Res. 39, 1340. http://dx.doi.org/10.1029/2002WR001952.

Michaud, J.D., Hirschboeck, K.K., Winchell, M., 2001. Regional variations in small-basin floods in the United States. Water Resour. Res. 37, 1405–1416.

NWS, 2014. Annual Flood Loss Summary Reports [WWW Document]. URL: http://www.nws.noaa.gov/hic/summaries/.

O'Connor, J.E., Costa, J.E., 2004. Spatial distribution of the largest rainfall-runoff floods from basins between 2.6 and 26,000 km^2 in the United States and Puerto Rico. Water Resour. Res. 40, W01107. http://dx.doi.org/10.1029/2003WR002247.

Ortega, K.L., Smith, T.M., Manross, K.L., Kolodziej, A.G., Scharfenberg, K.A., Witt, A., Gourley, J.J., 2009. The severe hazards analysis and verification experiment. Bull. Am. Meteorol. Soc. 90, 1519–1530. http://dx.doi.org/10.1175/2009BAMS2815.1.

Perucca, L.P., Angilieri, Y.E., 2011. Morphometric characterization of del Molle Basin applied to the evaluation of flash floods hazard, Iglesia Department, San Juan, Argentina: quaternary landscape evolution: interplay of climate, tectonics, geomorphology, and natural hazards. Quat. Int. 233, 81–86. http://dx.doi.org/10.1016/j.quaint.2010.08.007.

Saharia, M., Kirstetter, P.-E., Vergara, H., Gourley, J.J., Hong, Y., Giroud, M., 2016. Mapping flash flood severity in the United States. J. Hydrometeorol. http://dx.doi.org/10.1175/JHM-D-16-0082.1.

Schumm, S.A., 1956. Evolution of drainage systems and slopes in Badlands at Perth Amboy, New Jersey. Geol. Soc. Am. Bull. 67, 597–646. http://dx.doi.org/10.1130/0016-7606(1956) 67[597:EODSAS]2.0.CO;2.

Smith, J.A., 1992. Representation of basin scale in flood peak distributions. Water Resour. Res. 28, 2993–2999. http://dx.doi.org/10.1029/92WR01718.

Smith, K., Ward, R., 1998. Floods: Physical Processes and Human Impacts.

Villarini, G., Smith, J.A., 2010. Flood peak distributions for the eastern United States. Water Resour. Res. 46, W06504. http://dx.doi.org/10.1029/2009WR008395.